

# Controllable Frequency Entanglement via Auto-Phase-Matched Spontaneous Parametric Down-Conversion

Zachary D. Walton,\* Mark C. Booth, Alexander V. Sergienko, Bahaa E. A. Saleh, and Malvin C. Teich  
*Quantum Imaging Laboratory, Departments of Electrical & Computer Engineering and Physics,  
 Boston University, 8 Saint Mary's Street, Boston, Massachusetts 02215-2421*

A new method for generating entangled photons with controllable frequency correlation via spontaneous parametric down-conversion (SPDC) is presented. The method entails initiating counter-propagating SPDC in a single-mode nonlinear waveguide by pumping with a pulsed beam perpendicular to the waveguide. The method offers several advantages over other schemes, including the ability to generate frequency-correlated photon pairs regardless of the dispersion characteristics of the system. Numerical evidence demonstrates the improvement provided by this source in the special case of frequency-correlated two-photon states.

PACS numbers: 42.65.-k, 42.50.Dv, 03.65.Ud, 03.67-a

Spontaneous parametric down-conversion (SPDC) is a convenient process for generating pairs of photons that are entangled in one or more of their respective degrees of freedom (direction, frequency, polarization). This entanglement can be used to demonstrate counter-intuitive features of quantum mechanics and to implement the growing suite of quantum information technologies [1]. In a typical down-conversion experiment, a photon from a monochromatic pump beam decays into two photons (often referred to as signal and idler) via interaction with a nonlinear optical crystal. While the signal and idler may be broadband individually, conservation of energy requires that the sum of their respective frequencies equals the single frequency of the monochromatic pump. This engenders frequency anti-correlation in the down-converted beams. Aside from the frequency-anti-correlated case, the frequency-correlated and frequency-uncorrelated cases were also investigated theoretically by Campos et al. in 1990 [2]. At that time, neither a method of creating these novel states nor a practical application of the states was known.

Two developments in quantum information theory have renewed interest in these generalized states of frequency correlation. First, quantum information processes requiring the synchronized creation of multiple photon pairs have been devised, such as quantum teleportation [3] and entanglement swapping [4]. The requisite temporal control can be achieved by pumping the crystal with a brief pulse. The availability of pump photons of differing frequencies relaxes the strict frequency anti-correlation in the down-converted beams [5]. Second, applications such as entanglement-enhanced clock synchronization [6] and one-way auto-compensating quantum cryptography [7] have been introduced that specifically require frequency correlation, as opposed to the usual frequency anti-correlation.

Methods for preparing these novel states of frequency correlation have emerged as well. Keller and Rubin were first to observe that when a specific relationship between the group velocities of the pump and down-

converted beams holds, the down-converted photons are anti-correlated in time [5]. Using a first-order Taylor approximation of the relevant dispersion curves, they provided two examples of bulk nonlinear crystals that satisfied this relationship when used in a collinear type-II configuration (signal and idler orthogonally polarized). Erdmann et al. pointed out that the time-anti-correlated state described by Keller and Rubin entails frequency correlation (which can be seen immediately by Fourier duality), and further emphasized that perfect frequency correlation requires an infinite crystal, just as perfect frequency anti-correlation requires a pump with an infinite coherence length [8]. More recently, Giovannetti et al. demonstrated the feasibility of frequency-correlated down-conversion in a periodically-poled nonlinear crystal [9] and presented a formalism for parameterizing the space of states between the cases of perfect frequency correlation and perfect frequency anti-correlation [10].

In this Letter, we present a new method for obtaining controllable frequency entanglement that has distinct advantages over the previously proposed methods. Our method entails initiating type-I SPDC (signal and idler identically polarized) in a single-mode nonlinear waveguide by pumping with a pulsed beam perpendicular to the waveguide (see Fig. 1). The down-converted photons emerge from opposite ends of the waveguide with a joint spectrum that can be varied from frequency anti-correlated to frequency correlated by adjusting the temporal and spatial characteristics of the pump beam. The primary advantage of this method is that the limiting cases of perfect frequency correlation and perfect frequency anti-correlation can be obtained regardless of the dispersion relation of the waveguide. Thus, we refer to the method as *auto-phase-matched*. It is well known that the frequency-anti-correlated case is achievable regardless of the dispersion relations in a collinear configuration with a monochromatic pump and a thin bulk crystal; however, the frequency-correlated case has hitherto been associated with a constraint on the dispersion relations (cf. the “group velocity matching” condition introduced

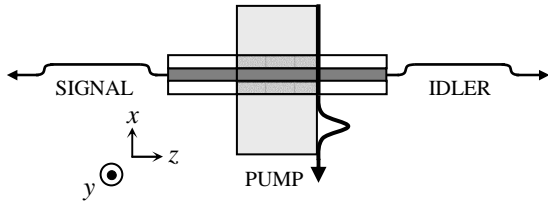


FIG. 1: A schematic of auto-phase-matched SPDC, a new method for generating entangled-photon pairs with controllable frequency correlation. The z-polarized pulsed pump beam initiates counter-propagating y-polarized SPDC in the single-mode nonlinear waveguide. The joint spectrum of the down-converted beams is controlled by the spatial and temporal characteristics of the pump beam, as described in the text.

in Ref. [5]). The geometry we propose restores the symmetry between the two cases by ensuring the appropriate phase-matching regardless of the dispersion relation of the waveguide.

This Letter is organized as follows. First, we derive the output state of the SPDC produced in our new configuration. Second, we analyze the state using a Franson interferometer [11], which illustrates the duality between frequency correlation and anti-correlation. Third, we quantify our method's advantage by comparing the visibility achieved in a Franson interferometer by the frequency-correlated, collinear configuration described in Ref. [9] with the visibility achieved by the same crystal used in our counter-propagating configuration.

The counter-propagating geometry depicted in Fig. 1 has been noted as a promising source of entangled-photon pairs for both type-I [12] and type-II [13] SPDC; however, these investigations were limited to the case of a monochromatic pump beam. Two primary beneficial effects are achieved by pumping with a broadband beam perpendicular to the waveguide and arranging for type-I down-conversion. First, the dispersion relation for the pump beam plays no role in the phase-matching analysis, since the waveguide ensures phase-matching in the transverse direction. Second, the counter-propagating, identically-polarized signal and idler fields will be phase-matched in the long-crystal limit only if they have equal and opposite propagation vectors, a condition which entails equal frequency. Thus, the bandwidth of the pump determines the allowable range of the sum frequency of the signal and idler, and the longitudinal length of the illuminated portion of the crystal determines the allowable range of the difference frequency.

We assume that the nonlinear coefficient and the propagation constants vary sufficiently slowly with frequency that they may be taken outside any frequency integrals in which they appear as integrand prefactors. Furthermore, we assume that the waveguide is long compared to the width of the pump beam such that the interaction length is controlled by the pump beam profile along the

z-axis (see Fig. 1). Following the standard procedure for deriving the quantum state that describes the counter-propagating photon pair (see, for example, Ref. [12]), we have

$$|\Psi\rangle \propto \iint d\omega_l d\omega_r \tilde{E}_t(\omega_l + \omega_r) \tilde{E}_z[\Delta\beta(\omega_l, \omega_r)] |\omega_l\rangle_l |\omega_r\rangle_r, \quad (1)$$

where  $\tilde{E}_t(\omega)$  and  $\tilde{E}_z(\Delta\beta)$  are the respective Fourier transforms of the temporal and spatial functions describing the pump beam  $E_p(t, z) = E_t(t)E_z(z)$ ,  $\Delta\beta(\omega_l, \omega_r) = \beta(\omega_l) - \beta(\omega_r)$  is the difference in the waveguide propagation constant evaluated at  $\omega_l$  and  $\omega_r$ , and  $|\omega\rangle_{l(r)}$  denotes a single photon at frequency  $\omega$  moving to the left(right). We will suppress all normalization coefficients; the efficiency of this geometry is shown in Ref. [13] to be approximately the same as the more conventional collinear-waveguide SPDC [14].

In the limit of monochromatic pump and short interaction length, the phase mismatch function  $\Delta\beta(\omega_l, \omega_r)$  may take on a wide range of values while the sum frequency of the signal and idler is fixed. This is the familiar frequency-anti-correlated case that is readily achievable in thin bulk crystals. In the broadband-pump long-interaction-length limit,  $\Delta\beta(\omega_l, \omega_r)$  is tightly distributed around 0, forcing  $\omega_l = \omega_r$  regardless of the waveguide's dispersion relation. The frequency of each down-converted beam is centered at half the center frequency of the pump and ranges over half the bandwidth of the pump. This is the frequency-correlated case that has hitherto only been achieved by imposing a condition on the crystal's dispersion relations at specific wavelengths.

The Franson interferometer [11] is a natural tool for distinguishing frequency correlation and frequency anti-correlation [18]. When the two delays ( $\tau_1$  and  $\tau_2$ ) are equal to within the reciprocal bandwidth of down-conversion, coincidence detections can be associated with indistinguishable pair-creation events (see Fig. 2A). If the down-converted photons are correlated in time (anti-correlated in frequency), the short-short two-photon amplitude interferes with the long-long amplitude (see Fig. 2B). If the down-converted photons are anti-correlated in time (correlated in frequency), the short-long amplitude interferes with the long-short amplitude (see Fig. 2C). The duality between these two cases can be seen by comparing the loci of indistinguishable pair-creation events in the spacetime diagrams of Fig. 2B and Fig. 2C. The frequency-anti-correlated case depicted in Fig. 2B arises from the coherent superposition of pair-creation events at a fixed position over a range of times, while the frequency-correlated case depicted in Fig. 2C arises from the coherent superposition of pair-creation events at a fixed time over a range of positions. Note that while the interference visibility decreases in both cases as  $\tau_1 - \tau_2$  approaches the reciprocal bandwidth of down-conversion, the relative phase between the interfering amplitudes depends on  $\tau_1 + \tau_2$  in the frequency-anti-

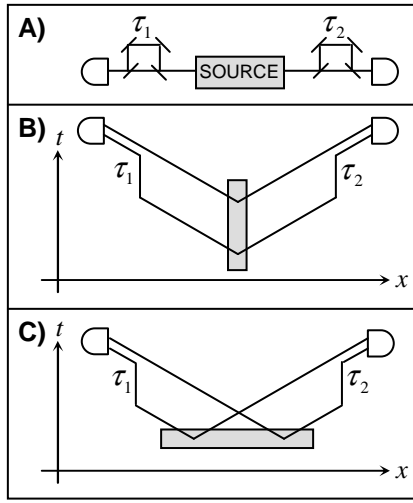


FIG. 2: The Franson interferometer (A) and the two types of indistinguishability it can bring about. B) depicts the indistinguishability in time of creation of the photon pair, and C) depicts indistinguishability in position of creation of the photon pair. These two cases are shown in the text to correspond to frequency-anti-correlated photon pairs and frequency-correlated photon pairs, respectively.

correlated case, and on  $\tau_1 - \tau_2$  in the frequency-correlated case.

In Fig. 3 we plot the probability of coincidence in the Franson interferometer for two limiting cases of the two-photon source: perfect frequency anti-correlation ( $\tilde{E}_t(\omega) \propto \delta(\omega - \omega_p)$ ,  $\tilde{E}_z(\Delta\beta)$  is a Gaussian centered at  $\Delta\beta = 0$ ) and perfect frequency-anti-correlation ( $\tilde{E}_z(\Delta\beta) \propto \delta(\Delta\beta)$  and  $\tilde{E}_t(\omega)$  is a Gaussian centered at  $\omega = \omega_p$ ). The widths of Gaussians are chosen such that the bandwidth of downconversion is  $\omega_p/10$  in each case. The fourth-order fringes in the  $\tau_1 \approx \tau_2 \gg 10/\omega_p$  region show that the Franson interferometer clearly distinguishes the two cases. The modulation is in the  $\Delta\tau_1 = \Delta\tau_2$  direction the frequency-anti-correlated case and in the  $\Delta\tau_1 = -\Delta\tau_2$  direction in the frequency-correlated case [19].

By establishing the signature of the perfect frequency-correlated state (the fourth-order fringes in Fig. 3B), we are able to compare the performance of experimental methods designed to produce this state. Specifically, the visibility of the fringes in Fig. 3B provides a measure of the quality of the frequency-correlated state. In Fig. 4 we plot a numerical calculation of the visibility achieved by the source described in Ref. [9] (thin line) and that achieved by our auto-phase-matched method (thick line) using the same crystal, for a range of interaction lengths. In the method of Ref. [9] the interaction length is the thickness of the crystal, while in our method the interaction length is the width of the pump beam in along the  $z$ -axis (see Fig. 1). In order to minimize the complicating effect of second-order interference, the visibility

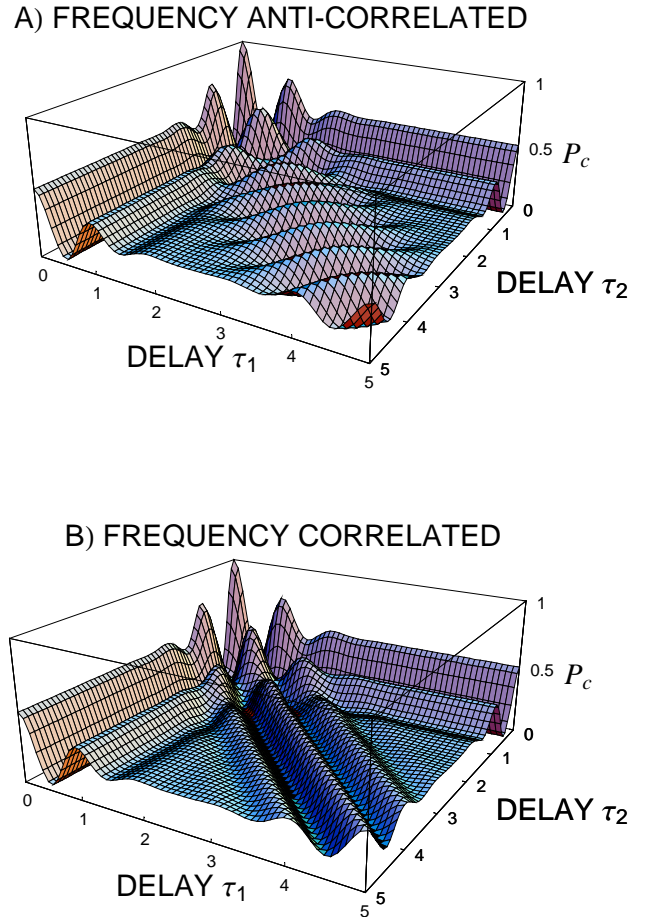


FIG. 3: The probability of coincidence when frequency-anti-correlated (A) and frequency-correlated (B) states are analyzed with a Franson interferometer. The down-converted beams have center frequency  $\omega_p/2$  and bandwidth  $\omega_p/10$ .  $\tau_1$  and  $\tau_2$  are in units of optical cycles at the center frequency of downconversion.

is calculated at the delay offset  $(\tau_1, \tau_2) = (4/\sigma, 4/\sigma)$  where  $\sigma$  is the bandwidth of down-conversion. While the fourth-order visibility in Fig. 3B is 0.5, we have scaled the visibilities to range between 0 and 1 in Fig. 4 since there exist well-known techniques for restoring maximal visibility (see, for example, Refs. [15, 16]).

The parameters of the source described in Ref. [9] are as follows: periodically-poled potassium titanyl phosphate (PPKTP) with a poling period of  $47.7 \mu\text{m}$ , pump wavelength of 790 nm, pump bandwidth of 3 THz, and collinear propagation along the crystal's  $x$  axis with the signal  $z$ -polarized and the pump and idler  $y$ -polarized. We adapt this crystal for our method by considering a slab KTP waveguide which is  $1 \mu\text{m}$  in the transverse dimension, surrounded by air, unpoled, and configured as depicted in Fig. 1 with the pump  $z$ -polarized and the signal and idler  $y$ -polarized. Since both schemes rely on a long-crystal phase-matching condition, it is not surprising that the visibility of each increases with increasing

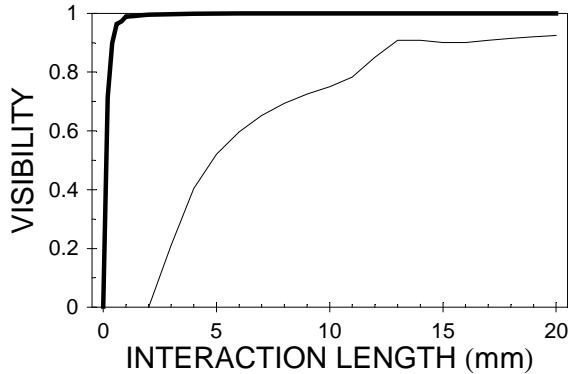


FIG. 4: Numerical calculation of the fourth-order fringe visibility seen in a Franson interferometer when the perfect source of frequency-correlated photon pairs is approximated by the method described in Ref. [9] (thin line) and by the auto-phase-matched method described in the text (bold line). The plot depicts the effect of changing the interaction length of the nonlinear process while holding the bandwidth of the pump fixed.

crystal length; however, while the deleterious influence of higher-order terms in the crystal dispersion relations is exacerbated as the crystal length is increased in the method of Ref. [9], our auto-phase-matched approach provides an increasingly close approximation to the desired state, regardless of the dispersion relations.

Finally, it is worth noting that our source may be used to create photon pairs that are entangled in polarization. In Fig. 1, we were only concerned with down-converted photons polarized along the  $y$ -axis. If the pump beam is polarized along the  $z$ -axis and we use a crystal like KTP which has  $\chi_{zxy}^{(2)} = \chi_{zyx}^{(2)} = 0$  and  $\chi_{zxx}^{(2)} \approx \chi_{zyy}^{(2)}$ , we will get a counter-propagating polarization entangled state ( $|HH\rangle + e^{i\phi}|VV\rangle$ , where  $\phi$  is related to the crystal birefringence) directly from the crystal. Furthermore, we can obtain this polarization-entanglement while independently controlling the frequency entanglement by manipulating the pump beam, as previously described.

This work was supported by the National Science Foundation; the Center for Subsurface Sensing and Imaging Systems (CenSSIS), an NSF Engineering Research Center; the Defense Advanced Research Projects Agency (DARPA); and the David and Lucile Packard Foundation.

and *Quantum Information* (Cambridge University Press, Cambridge, 2001).

- [2] R. A. Campos, B. E. A. Saleh, and M. C. Teich, Phys. Rev. A **42**, 4127 (1990).
- [3] C. H. Bennett, G. Brassard, C. Crépeau, R. Jozsa, A. Peres, and W. K. Wootters, Phys. Rev. Lett. **70**, 1895 (1993).
- [4] J. W. Pan, D. Bouwmeester, H. Weinfurter, and A. Zeilinger, Phys. Rev. Lett. **80**, 3891 (1998).
- [5] T. E. Keller and M. H. Rubin, Phys. Rev. A **56**, 1534 (1997).
- [6] V. Giovannetti, S. Lloyd, and L. Maccone, Nature **412**, 417 (2002).
- [7] Z. Walton, A. F. Abouraddy, A. V. Sergienko, B. E. A. Saleh, and M. C. Teich, quant-ph/0207167 (2002).
- [8] R. Erdmann, D. Branning, W. P. Grice, and I. A. Walmsley, Phys. Rev. A **62**, 53810 (2000).
- [9] V. Giovannetti, L. Maccone, J. H. Shapiro, and F. N. C. Wong, Phys. Rev. Lett. **88**, 183602 (2002).
- [10] V. Giovannetti, L. Maccone, J. H. Shapiro, and F. N. C. Wong, quant-ph/0207009 (2002).
- [11] J. D. Franson, Phys. Rev. Lett. **62**, 2205 (1989).
- [12] M. C. Booth, M. Atatüre, G. Di Giuseppe, A. V. Sergienko, B. M. Jost, B. E. A. Saleh, and M. C. Teich, Phys. Rev. A (2002), in press.
- [13] A. D. Rossi and V. Berger, Phys. Rev. Lett. **88**, 043901 (2002).
- [14] S. Tanzilli, H. D. Riedmatten, W. Tittel, H. Zbinden, P. Baldi, M. D. Michel, D. B. Ostrowsky, and N. Gisin, Electron. Lett. **37**, 26 (2001).
- [15] J. Brendel, E. Mohler, and W. Martienssen, Phys. Rev. Lett. **66**, 1142 (1991).
- [16] D. V. Strekalov, T. B. Pittman, A. V. Sergienko, Y. H. Shih, and P. G. Kwiat, Phys. Rev. A **54**, R1 (1996).
- [17] C. K. Hong, Z. Y. Ou, and L. Mandel, Phys. Rev. Lett. **59**, 2044 (1987).
- [18] Previous authors analyzing generalized frequency entanglement have used a beamsplitter and a Mach-Zehnder interferometer to compare the frequency-correlation and frequency-anti-correlation cases (see, for example, [2, 9]). These efforts are complicated by the fact that the indistinguishability of pair-creation events is conflated with reflect-reflect/transmit-transmit Feynman-path indistinguishability. The confusion of these distinct types of interference has led some to claim that a photon pair must be entangled for the Hong-Ou-Mandel “dip” [17] to appear. In fact, Campos et al. showed in their 1990 work [2] that a frequency-uncorrelated source will also produce a null in coincidence after a beam splitter when the input path lengths are equal.
- [19] It is interesting to note that the absence of modulation along the  $\tau_1 = \tau_2$  axis in the frequency-correlated case is the source of the insensitivity to interferometric drift in the one-way autocompensating quantum cryptography scheme recently discovered [7]. The insensitivity arises because the two photons are time-multiplexed over the same Mach-Zehnder interferometer; thus, drift in the optical delay is equivalent to moving along the line  $\tau_1 = \tau_2$  in Fig. 3B.

\* Electronic address: walton@bu.edu; Quantum Imaging Laboratory homepage: <http://www.bu.edu/qi1>

[1] M. A. Nielsen and I. L. Chuang, *Quantum Computing*